Journal of Materials Chemistry A

Accepted Manuscript

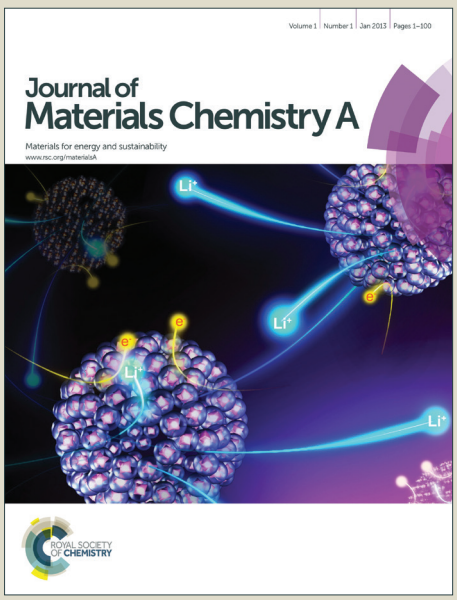

ROYAL SOCIETY OF CHEMISTRY

www.rsc.org/materialsA

Journal Name

COMMUNICATION

Decoration of Co/Co_3O_4 nanoparticles with Ru nanoclusters: A new strategy for design of highly-active hydrogenation

Received 00th January 20xx,
Accepted 00th January 20xx

DOI: 10.1039/x0xx00000x

www.rsc.org/

Lihua Zhu,[a] Zhiqing Yang,[b,*] Jinbao Zheng,[a] Weiwei Hu,[b] Nuowei Zhang,[a] Yunhua Li,[a] Chuan-Jian Zhong,[c] Hengqiang Ye[b] and Binghui Chen[a,*]

$Ru/Co/Co_3O_4/C$ (Ru nanoclusters-on-Co/Co_3O_4 nanoparticles) has an unexpected enhancement of activity for benzene hydrogenation which is about 2500 times higher than Ru-Co nanoalloy/C. Detailed nanostructure characterizations of $Ru/Co/Co_3O_4/C$ have revealed that the high activity originates from a synergetic multifunction of the catalytic Ru, Co and Co_3O_4 sites on the nanocluster/nanoparticle surfaces.

To meet the increasing demand for diesel fuels there is a clear need to develop efficient catalysts for removing aromatic compounds in diesel fuels which constitute a major source of air pollution.[1,2] Among various catalysts for aromatic hydrogenation reaction, nickel-based,[3] platinum-based,[4,5] ruthenium-based,[6-12] iridium-based,[13,14] rhodium-based[15] and bimetallic catalysts (Pd-Rh,[16] La-Ni,[17] Pt-Pd,[18] Rh-Pt, Ir-Pt, Ru-Pt[19] and Au-Pd[20]) have been widely used. Non-noble metal catalysts are cheap to some extent, but their catalytic activity, selectivity and stability are generally poorer than noble metal catalysts. It is highly desirable to develop low-cost and highly-efficient catalysts for aromatic hydrogenation reaction under relatively mild conditions.

To that end, a an important strategy is to design the catalysts with synergistically multifunctional active sites, which plays a vital role in the heterogeneous catalysis.[21-24] For instance, Song and co-workers[25] have proved that Lewis acidic ionic liquid ([bmim]Cl-$AlCl_3$) and Pd/C could work cooperatively to improve arenes hydrogenation. The cooperation of multiple active sites has been also utilized in the Rh(cod)-Pd/SiO_2 catalyst for benzene hydrogenation[26] and in the Rh-CNR_2/Pd-SiO_2 catalyst for the hydrogenation of toluene to methylcyclohexane.[27]

Herein we report a new strategy to design and prepare a nanocluster-decorated nanoparticle catalyst with multiple active sites by a combination of noble metal nanoclusters and transition metal oxide nanoparticles (NM-TM/TMO). This strategy is exemplified via the design of $Ru/Co/Co_3O_4/C$, where Ru nanoclusters are anchored to the surface of Co/Co_3O_4 nanoparticles (NPs) supported on carbon black. For benzene hydrogenation as a model reaction, we hypothesize a synergetic multifunction of the catalytic sites in three surface processes (Scheme 1), including Ru sites for activation of molecular hydrogen (Process 1), Co_3O_4 sites (P-type semiconductor with positively charged holes) for activation of benzene (with pi-electron) via electrophilic adsorption (Process 2), and Co sites acting as a "bridge" for transferring the activated H species to the activated benzene by hydrogen spillover process (Process 3). We demonstrate that the cooperation of Ru, Co and Co_3O_4 sites in these processes can effectively enhance the catalytic performance of the catalyst for benzene hydrogenation reaction, which constitute a new strategy for the design of highly-active catalysts at atomic level.

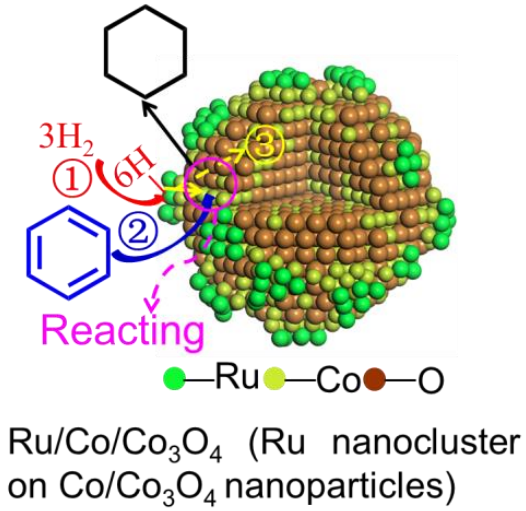

Scheme 1 The design of a novel multifunctional catalyst consisting of Ru nanoclusters decorated Ni/NiO nanoparticles (Ru-Ni/NiO) supported on carbon for benzene hydrogenation.

[a] Department of Chemical and Biochemical Engineering, National Engineering Laboratory for Green Productions of Alcohols-Ethers-Esters, College of Chemistry and Chemical Engineering, Xiamen University, Xiamen 361005, China. E-mail: chenbh@xmu.edu.cn; Fax: (+) 86-592-2184822.
[b] Shenyang National Laboratory for Materials Science, Institute of Metal Research, Chinese Academy of Sciences, Shenyang 110016, China. yangzq@imr.ac.cn.
[c] Department of Chemistry, State University of New York at Binghamton, Binghamton, New York 13902, United States.

† Electronic Supplementary Information (ESI) available: Synthetic details, BET, TG, XRD, some TEM, HRTEM, HAADF-STEM images, elemental mapping and schematic models of the catalysts, and catalytic performance of the catalysts reported in the literatures,. See DOI: 10.1039/x0xx00000x

$Co/Co(OH)_2/C$ was prepared at RT via a hydrazine hydrate reduction method, similar to the synthesis of $Ni/Ni(OH)_2/C$.[28,29] $Ru/Co/Co(OH)_2/C$ was obtained by galvanic replacement method.[30-32] After $Co/Co(OH)_2/C$ and $Ru/Co/Co(OH)_2/C$ were annealed in flowing N_2 of 80 mL min^{-1} at 280 ℃ for 3 h, producing $Co/Co_3O_4/C$ and $Ru/Co/Co_3O_4/C$, respectively. For comparison, Ru-Co/C catalyst was obtained after $Ru/Co/Co(OH)_2/C$ reduced in N_2+10%H_2 of 80 mL min^{-1} at 280 ℃ for 3 h and Ru/C was prepared via impregnation method (Scheme S1 and experimental details in Supporting Information).

TG results provided strong evidence for the formation of cobaltosic oxide (Co_3O_4) after calcining $Ru/Co/Co(OH)_2/C$ in N_2 at 280 ℃ (Fig. S1). The textural properties of different samples are similar (Table S1). The mesoporous characteristic is evidenced by the nitrogen adsorption-desorption isotherm for $Ru/Co/Co_3O_4/C$ (Fig. S2). There is no characteristic diffraction peak for Ru metal in the XRD patterns for $Ru/Co/Co_3O_4/C$ (Fig. S3A), indicating that Ru are either very small or amorphous in this catalyst. And the formation of Ru-Co nanoalloy is confirmed in the Ru-Co/C catalyst (Fig. S3B). The $Co/Co_3O_4/C$, Ru/C and $Ru/Co/Co_3O_4/C$ catalysts display a mean particle size of 2~3 nm with a quite narrow size distribution and high dispersity (Fig. S4).

Fig. 1 displays a typical set of HRTEM images for the $Co/Co_3O_4/C$, Ru/C, $Ru/Co/Co_3O_4/C$ and Ru-Co/C samples. The $Co/Co_3O_4/C$ sample (Fig. 1a) shows a lattice fringe of 0.233 nm, which corresponds to the (222) facets of Co_3O_4 with face-centered cubic (fcc) structure. As shown in Fig. 1b, the indicated lattice fringes with interplanar spacing of 0.213 nm could be ascribed to Ru (002) planes.[33] Fig. 1c displays lattice fringes with a distance of 0.233 nm, assigned to the (222) facets of Co_3O_4, indicating that Co element is mainly with the form of Co_3O_4 in the $Ru/Co/Co_3O_4/C$ sample. Ru nanoclusters are highly dispersed and too small. Ru cannot be observed in the HRTEM images for most of the $Ru/Co/Co_3O_4$ bimetallic nanoparticles (BNPs). However, after the $Ru/Co/Co(OH)_2/C$ was treated in N_2+10%H_2 at 280 ℃, the lattice fringe was reduced to 0.223 nm (Fig. 1d), which is smaller than Ru(100)-0.238 nm[34] and larger than Co(111)-0.205 nm, demonstrating the Ru-Co nanoalloy characteristic.

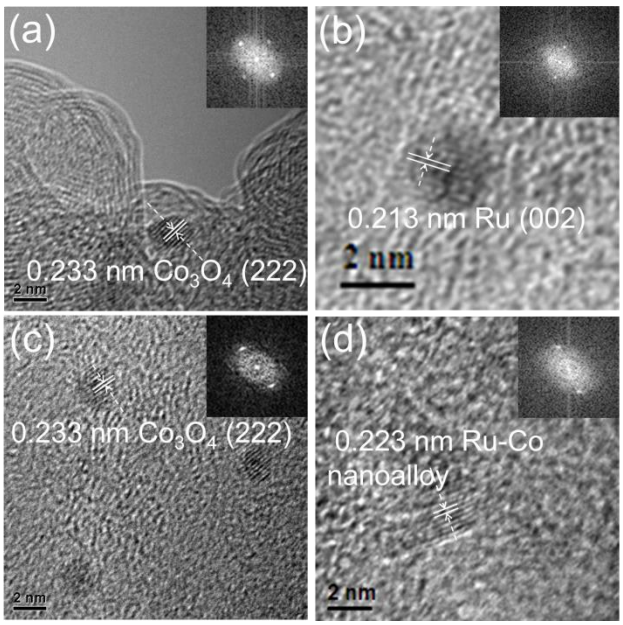

Fig. 1 HRTEM images for (a) $Co/Co_3O_4/C$, (b) Ru/C, (c) $Ru/Co/Co_3O_4/C$ and (d) Ru-Co/C sample. The insets show their respective fast Fourier transform (FFT) patterns results.

The nanostructures and elemental distributions of the $Ru/Co/Co_3O_4/C$ and Ru-Co/C catalysts were measured by high angle annular dark-field scanning transmission electron microscopy (HAADF-STEM) in combination with energy dispersive X-ray spectroscopy (EDS). Fig. 2 shows a typical HAADF-STEM image and corresponding elemental mapping results for the $Ru/Co/Co_3O_4/C$ catalyst. The bright particles exhibit an average diameter of about 2.0 nm. There are many isolated bright particles in the HAADF-STEM image, demonstrating the presence of NPs composed of heavier elements dispersed on the carbon matrix. Ru, Co and O were detected from the bright NPs on carbon matrix by EDS, as shown in Fig. 2b. The low EDS counts make it hard to quantify the concentration of Ru and Co in the NPs. Fig. 2c,d are elemental maps for Ru and Co recorded using the Ru L-peak (~2.56 keV) and Co K-peak (~6.93 keV), respectively. It is clear that those brighter NPs are Ru-rich, based on analysis of the HAADF-STEM image and the Ru mapping data (Fig. 2a,c). In comparison with the positions of the four local regions with relatively higher Co concentration highlighted by white circles in the Co map (Fig. 2d) in the Ru map (Fig. 2c), the centers of Co-rich regions are found to deviate slightly from those of Ru-rich regions (Fig. 2e), demonstrating the presence of isolated Ru-rich nanoclusters immediately adjacent to those Co-rich ones. The nanostructure of the $Ru/Co/Co_3O_4$ NPs is vividly depicted by atomic model in Fig. 2f. These results are consistent with EDS elemental line-scan results for Ru, Co, O and C across several $Ru/Co/Co_3O_4$ BNPs (Fig. S5).

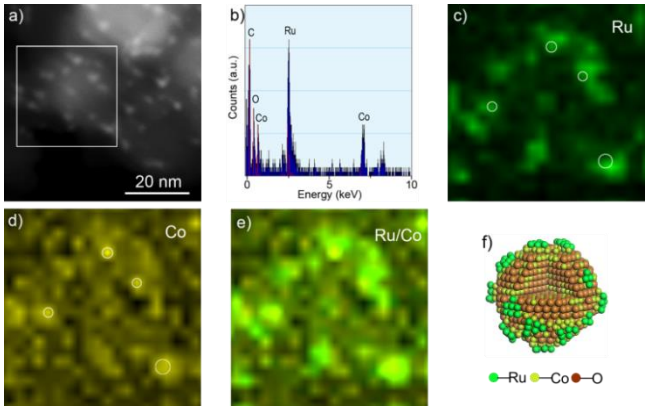

Fig. 2 HAADF-STEM image and EDS measurements of individual BNPs for the $Ru/Co/Co_3O_4/C$ sample. a) HAADF-STEM image. b) An EDS spectrum acquired from a bright NP. c), d) and e) elemental maps for Ru (green), Co (yellow) and Ru versus Co for the selected square region in the HAADF-STEM image, respectively. f) The atomic model of the $Ru/Co/Co_3O_4$ BNPs in the $Ru/Co/Co_3O_4/C$ sample.

Fig. 3a shows a HAADF-STEM image for the Ru-Co/C sample and corresponding EDS line-scan results for Ru, Co, O and C across several particles. The size of some particles in the Ru-Co/C sample is above 10 nm which is much larger than $Ru/Co/Co_3O_4$ BNPs, with agglomeration of NPs to some extent. It indicates that strong interactions between Ru nanoclusters and Co/Co_3O_4 NPs are important for stabilizing Ru nanoclusters on Co/Co_3O_4 for $Ru/Co/Co_3O_4/C$. The fact that EDS counts for Co change in a way similar to that for Ru in all the measured particles, irrespective of the size and shape of the particles (Fig. 3b,c) strongly suggests that Co and Ru are likely mixed to form Ru-Co nanoalloy in the Ru-Co/C sample (consistent with the XPS results in Fig. S6).

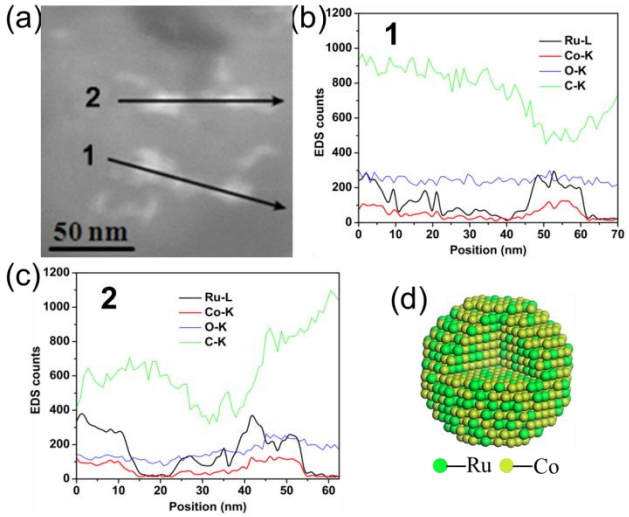

Fig. 3 (a) HAADF-STEM images for the Ru-Co/C sample. (b) and (c) composition line profiles obtained by energy-dispersive X-ray spectroscopy (EDS) with an electron beam scanning across individual Ru-Co BNPs along the arrow direction, black (Ru), red (Co), green (C) and blue (O). (d) The atomic model of the Ru-Co NPs in the Ru-Co/C sample.

The outmost atomic compositions of the $Co/Co_3O_4/C$, Ru/C, $Ru/Co/Co_3O_4/C$ and Ru-Co/C samples were obtained by high-sensitivity low-energy ion scattering (HS-LEIS) measurements. Fig. 4a,b indicate that Co atoms exist on the outermost atom layer of the $Co/Co_3O_4/C$ sample and Ru atoms are present on the outmost surface of the Ru/C sample. For the $Ru/Co/Co_3O_4/C$ and Ru-Co/C catalysts (Fig. 4c,d), Ru and Co atoms co-exist on the outmost surface, but the intensity of Ru peak is much larger on the outer surface of $Ru/Co/Co_3O_4/C$ than on that of Ru-Co/C. Therefore, it is likely that the number of Ru atoms on the surface of the $Ru/Co/Co_3O_4$ BNPs is much larger than that on the surface of the Ru-Co BNPs. The different atom-scale structures of the catalysts are schematically illustrated by atomic models of BNPs in Fig. 4 and Scheme S2.

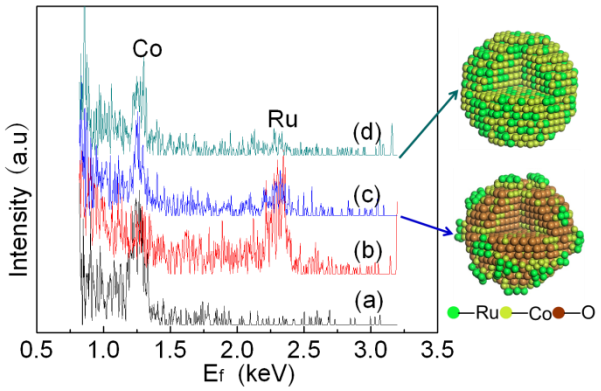

Fig. 4 5 keV $^{20}Ne^+$ HS-LEIS spectra for (a) $Co/Co_3O_4/C$, (b) Ru/C, (c) $Ru/Co/Co_3O_4/C$ (Ru nanocluster-on-Co/Co_3O_4) and (d) Ru-Co/C (Ru-Co nanoalloy) samples.

The catalytic activities of the different catalysts for benzene hydrogenation reaction are shown in Table 1. When this reaction was conducted under 5.3 MPa H_2 and 60 ℃, the $Ru/Co/Co_3O_4/C$ catalyst exhibited a 100% yield to cyclohexane and an unexpected high activity, with a TOF of 91051.5 h^{-1} (Table 1, entry 1) within 0.2 h, which was almost 2500 times more active than that of the Ru-Co/C catalyst with a TOF of 36.4 h^{-1} and a 0.2% yield toward cyclohexane within reaction time of 1 h (Table 1, entry 2). The reaction was also carried out over the $Co/Co_3O_4/C$ and Ru/C catalysts, it could be found that the catalytic activity of Ru/C (with a TOF of 1706.0 h^{-1} and a 9.42% yield) (Table 1, entry 3) and $Co/Co_3O_4/C$ (with a yield below 0.1%) was much lower than that of $Ru/Co/Co_3O_4/C$. For comparison, the reaction was also carried out over carbon, but it did not produce any product. Obviously, the Ru nanoclusters anchored on Co/Co_3O_4 catalyst was the most active for benzene hydrogenation to cyclohexane among the catalysts investigated in this study. It's worth mentioning that this $Ru/Co/Co_3O_4/C$ catalyst shows unexpected high catalytic property relative to most of the supported and unsupported Ru-based, Rh-based, Pd-based, Ir-based and bimetallic-based under similar reaction conditions (Table S2). Based on the above structural characterizations and catalytic performance testing results, important insights are gained into the structures responsible for the high catalytic performance of the $Ru/Co/Co_3O_4/C$ catalyst: 1) small Ru nanoclusters (about 1 nm) highly dispersed onto Co/Co_3O_4 surface, and 2) synergetic active sites (Ru, Co and Co_3O_4).

Table 1 Catalytic performance of the catalysts for benzene hydrogenation[a]

Entry	Catalyst	t (h)	TOF(h^{-1})	Yield to cyclohexane
1	$Ru/Co/Co_3O_4/C$	0.2	91051.5	100%
2	Ru-Co/C	1	36.4	0.2%
3	Ru/C	1	1706.0	9.4%

[a]Reaction conditions: benzene, 10 mL; H_2 pressure, 5.3 MPa; catalyst, 0.05 g; reaction temperature, 60 ℃. [b]TOF (turnover frequency) of the catalysts was calculated as: conversion of mols of benzene per mol of ruthenium per hour. Yields for $Co/Co_3O_4/C$ and carbon were < 0.1%.

The proposed mechanisms for benzene hydrogenation over the $Ru/Co/Co_3O_4/C$ and Ru-Co/C catalysts are shown in Scheme S3. Because Ru is much more active than Co for activating H_2, the process starts with the diffusion and adsorption of H_2 on the Ru active sites preferentially, rather than on the Co/Co_3O_4 surface. And the hydrogen dissociation occurs at Ru atom sites, forming activated-H species. With the positively charged benzene (with pi-electrons), negatively charged cobaltosic oxide (Co_3O_4-P-type semiconductor with positively charged holes) and the nanocluster Ru sites, benzene is easily adsorbed and activated at the Co_3O_4 sites via the electrophilic adsorption interaction between the π-electrons and holes. The activated-H species will transfer to the Co_3O_4 surface by spillover process.[35,36] Co sites in the central region of $Ru/Co/Co_3O_4$ BNP provide a "bridge" which transfers the activated H species to activated-benzene, producing cyclohexane. The cooperation of Ru, Co and Co_3O_4 sites effectively improves the catalytic performance of the $Ru/Co/Co_3O_4/C$ catalyst for benzene hydrogenation. For the Ru-Co/C catalyst where H_2 and benzene are adsorbed and activated at the same sites (Ru-Co nanoalloy), the absence of the synergetic effect of catalytic sites is responsible for the low catalytic activity.

In summary, $Ru/Co/Co_3O_4/C$-Ru nanoclusters anchored on Co/Co_3O_4 and Ru-Co nanoalloy/C catalysts were successfully designed and synthesized in this work. It is the unique atomic-scale

structural arrangement of Ru, Co and Co_3O_4 sites that is responsible for the catalytic synergy for the hydrogenation reactions. Exploration of this synergy is expected to provide a new and simple strategy for the design of the low level of noble metals and ultrahigh catalytic activity nanocatalysts for many other hydrogenation reactions.

Acknowledgements

The authors would like to thank the National Natural Science Foundation of China (Grant 201106118, 21303140, 51371189 and 51390473) for financial supports.

Notes and references

1 A. Stanislaus and B. H. Cooper, *Cat. Rev.*, 1994, **36**, 75–123.
2 B. H. Cooper and B. B. L. Donnis, *Appl. Catal. A*, 1996, **137**, 203–223.
3 R. J. White, R. Luque, V. L. Budarin, J. H. Clark and D. J. Macquarrie, *Chem. Soc. Rev.*, 2009, **38**, 481–494..
4 F. Domínguez, J. Sánchez, G. Arteaga and E. Choren, *J. Mol. Catal. A*, 2005, **228**, 319–324.
5 L. J. Simon, J. G. van Ommen, A. Jentys and J. A. Lercher, *J. Catal.*, 2001, **201**, 60–69.
6 A. Nowicki, Y. Zhang, B. Leger, J.-P. Rolland, H. Bricout, E. Monflier and A. Roucoux, *Chem. Commun.*, 2006, 296–298.
7 K. X. Yao, X. Liu, Z. Li, C. C. Li, H. C. Zeng and Y. Han, *ChemCatChem*, 2012, **4**, 1938–1942.
8 M. Zahmakiran and S. Özkar, *Langmuir*, 2008, **24**, 7065–7067.
9 J. M. Campelo, D. Luna, R. Luque, J. M. Marinas and A. A. Romero, *ChemSusChem*, 2009, **2**, 18–45.
10 S. Miao, Z. Liu, B. Han, J. Huang, Z. Sun, J. Zhang and T. Jiang, *Angew. Chem. Int. Ed.*, 2006, **45**, 266–269.
11 M. Zahmakıran, Y. Tonbul and S. Özkar, *J. Am. Chem. Soc.*, 2010, **132**, 6541–6549.
12 Y. Ma, Y. Huang, Y. Cheng, L. Wang and X. Li, *Appl. Catal. A*, 2014, **484**, 154–160.
13 V. Mévellec, A. Roucoux, E. Ramirez, K. Philippot and B. Chaudret, *Adv. Synth. Catal.*, 2004, **346**, 72–76.
14 Y. Tonbul, M. Zahmakiran and S. Özkar, *Appl. Catal. B*, 2014, **148–149**, 466–472.
15 C. Hubert, E. G. Bile, A. Denicourt-Nowicki and A. Roucoux, *Green. Chem.*, 2011, **13**, 1766–1771.
16 B. Yoon, H.-B. Pan and C. M. Wai, *J. Phys. Chem. C*, 2009, **113**, 1520–1525.
17 A. Louloudi and N. Papayannakos, *Appl. Catal. A*, 1998, **175**, 21–31.
18 B. Pawelec, V. La Parola, R. M. Navarro, S. Murcia-Mascarós and J. L. G. Fierro, *Carbon*, 2006, **44**, 84–98.
19 N. A. Dehm, X. Zhang and J. M. Buriak, *Inorg. Chem.*, 2010, **49**, 2706–2714.
20 A. M. Venezia, V. L. Parola, B. Pawelec and J. L. G. Fierro, *Appl. Catal. A*, 2004, **264**, 43–51.
21 Q. Fu, W.-X. Li, Y. Yao, H. Liu, H.-Y. Su, D. Ma, X.-K. Gu, L. Chen, Z. Wang, H. Zhang, B. Wang and X. Bao, *Science*, 2010, **328**, 1141–1144.
22 A. Villa, G. M. Veith and L. Prati, *Angew. Chem. Int. Ed.*, 2010, **49**, 4499–4502.
23 I. Lee, J. B. Joo, Y. Yin and F. Zaera, *Angew. Chem. Int. Ed.*, 2011, **50**, 10208–10211.
24 G. Kyriakou, M. B. Boucher, A. D. Jewell, E. A. Lewis, T. J. Lawton, A. E. Baber, H. L. Tierney, M. Flytzani-Stephanopoulos and E. H. Sykes, *Science*, 2012, **335**, 1209–1212.
25 R. R. Deshmukh, J. W. Lee, U. S. Shin, J. Y. Lee and C. E. Song, *Angew. Chem. Int. Ed.*, 2008, **47**, 8615–8617.
26 P. Barbaro, C. Bianchini, V. Dal Santo, A. Meli, S. Moneti, C. Pirovano, R. Psaro, L. Sordelli and F. Vizza, *Organometallics*, 2008, **27**, 2809–2824.
27 H. Gao and R. J. Angelici, *J. Am. Chem. Soc.*, 1997, **119**, 6937–6938.
28 L. Zhu, M. Cao, L. Li, Y. Tang, N. Zhang, J. Zheng, H. Zhou, Y. Li, L. Yang, C.-J. Zhong and B. H. Chen, *ChemCatChem*, 2014, **6**, 2039–2046.
29 L. Zhu, L. Zheng, K. Du, H. Fu, Y. Li, G. You and B. H. Chen, *RSC Adv.*, 2013, **3**, 713–719.
30 L Y. Li, L. Zhu, K. Yan, J. Zheng, B. H. Chen and W. Wang, *Chem. Eng. J.*, 2013, **226**, 166–170.
31 Y. Li, Q. Zhang, N. Zhang, L. Zhu, J. Zheng and B. H. Chen, *Int. J. Hydrogen Energy*, 2013, **38**, 13360–13367.
32 Y. Huang, Y. Ma, Y. Cheng, L. Wang and X. Li, *Ind. Eng. Chem. Res.*, 2014, **53**, 4604–4613.
33 G. Li, H. Nagasawa, M. Kanezashi, T. Yoshioka and T. Tsuru, *J. Mater. Chem. A*, 2014, **2**, 9185–9192.
34 C. Li, S. Zhang, B. Zhang, D. Su, S. He, Y. Zhao, J. Liu, F. Wang, M. Wei, D. G. Evansa and X. Duana, *J. Mater. Chem. A*, 2013, **1**, 2461–2467.
35 W. C. Conner and J. L. Falconer, *Chem. Rev.*, 1995, **95**, 759–788.
36 R. Prins, *Chem. Rev.*, 2012, **112**, 2714–2738.

Table of contents entry

Ru/Co/Co_3O_4/C (Ru nanoclusters-on-Co/Co_3O_4 nanoparticles) shows unexpected catalytic activity for benzene hydrogenation via the synergetic-effect of Ru, Co and Co_3O_4 sites.